Effect of Finite-rate Chemical Reactions on Turbulence in Hypersonic Turbulent Boundary Layers

Lian Duan* and M. Pino Martín†

Princeton University, Princeton, NJ, 08544

We conduct direct numerical simulations of reacting turbulent boundary layers to study the effects of finite-rate chemistry on turbulence as well as turbulence-chemistry interaction. It is found that turbulence fluctuations have a relative large influence on the dissociation reaction, while have a subtle influence on the recombination reaction. The influence of chemical reactions on temperature fluctuation variance, Reynolds stresses and turbulence kinetic energy is analyzed, and the results are compared with the non-reacting case. We find that the recombination reaction enhances turbulence, while the dissociation reaction damps turbulence. Chemical reactions influence the velocity field mainly by the heat of reaction, which causes volumetric flow expansion/contraction. The correlation of temperature fluctuation and fluctuation in species composition is significantly enhanced, and temperature fluctuations cause large fluctuations in species composition.

I. Introduction

The boundary layer on future air-breathing hypersonic cruise vehicles will be turbulent and chemically reacting. To aid the design of such vehicles, a greater understanding of turbulent hypersonic flows is needed. Although there has been significant progress in understanding and modeling turbulence and chemical reaction separately, the coupled behavior of turbulence and chemistry continues to present a challenging task and remains an active area of research.[1,2,3,4] The nonlinear interactions between turbulence and chemical reaction occur over a wide range of time and length scales and involves many different quantities. Our lack of adequate understanding of these interactions imposes serious limitations on modeling turbulence flows. For example, the majority of existent turbulence models which are used for reacting flow calculations are based on those developed for non-reacting flows, which are potentially limited.

Most of previous numerical and experimental investigations involving turbulence-chemistry interaction primarily discuss the influence of the coherence structures on mixing and reaction in mixing free shear flows.[5,6,7,8,9,10] These efforts are mainly focused on combustion applications since the free shear flows, especially mixing layers are considered the first step of most important combustion processes. The results of these investigations indicate the importance of large structure as well as small-scale structures on the mixing and reaction and show that these structures are significantly affected by the exothermicity of the reaction and the flow compressibility.

Mixing and reaction in homogeneous turbulence have also been the subject of numerous investigations.[11,12,13,14,15,16] For example, Martin and Candler[14] study turbulence-chemistry interaction via direct numerical simulation of reacting isotropic turbulence. Their results show that there is a positive feedback between the turbulence and exothermic reactions, and the feedback occurs through the pressure-strain term. Jaberi *et al.*[16] study the turbulence-chemistry interaction in homogeneous decaying compressible turbulence. Their results show that the pressure-dilatation tends to increase the turbulent kinetic energy when the reaction is exothermic.

There are few studies of turbulence-chemistry interaction for hypersonic boundary layers.[17,18,19] These flows are significantly different from turbulent combustion flows, which have been studied extensively. In hypersonic flows the dominant chemical reactions are the dissociation and recombination of nitrogen or oxygen molecules. The reactions have a high activation energy and the reaction rate is typically temperature

*Ph.D. Student, Department of Mechanical and Aerospace Engineering. AIAA Student Member.

†Assistant Professor, Department of Mechanical and Aerospace Engineering, AIAA Senior Member.

limited. In this case, small increases in the temperature result in large increases in reaction rate, which is contrasted with non-premixed combustion flows where the fuel-oxidizer mixing rate determines the rate of product formation and the reaction process is relatively insensitive to the temperature. Also, boundary layer flows are significantly different from idealized homogeneous turbulence or free shear layers due to the existence of the wall.

In this paper, we follow the approach by Martin & Candler.[17,18,19] The main objectives are (1) to analyze the different influence of turbulent fluctuations on dissociation and recombination reactions, (2) to study the combined effects of dissociation and recombination reactions on turbulent flow field, more specifically, temperature fluctuation variance, Reynolds stresses, turbulent kinetic energy and flow structures, and (3) to investigate the effects of turbulence-chemistry interaction.

II. Governing Equations

The equations describing the unsteady motion of a reacting fluid are given by the species mass, mass-averaged momentum, and total energy conservation equations, which, neglecting thermal non-equilibrium, are

$$\begin{aligned} \frac{\partial \rho_s}{\partial t} + \frac{\partial}{\partial x_j}\Big(\rho_s u_j + \rho_s v_{sj}\Big) &= w_s \\ \frac{\partial \rho u_i}{\partial t} + \frac{\partial}{\partial x_j}\Big(\rho u_i u_j + p\delta_{ij} - \sigma_{ij}\Big) &= 0 \\ \frac{\partial E}{\partial t} + \frac{\partial}{\partial x_j}\Big((E+p)u_j - u_i\sigma_{ij} + q_j + \sum_s \rho_s v_{sj} h_s\Big) &= 0 \end{aligned} \tag{1}$$

where w_s represents the rate of production of species s due to chemical reactions; ρ_s is the density of species s; u_j is the mass-averaged velocity in the j direction; v_{sj} is the diffusion velocity of species s; p is the pressure; σ_{ij} is the shear stress tensor, which is given by a linear stress-strain relationship; and E is the total energy per unit volume given by

$$E = \sum_s \rho_s c_{vs} T + \frac{1}{2}\rho u_i u_i + \sum_s \rho_s h_s^\circ, \tag{2}$$

where c_{vs} is the specific heat at constant volume of species s; and h° is the heat of formation of species s.

To derive the expression for w_s, consider a reaction where species $S1$ reacts to form species $S2$

$$S1 + M \rightleftharpoons S2 + M \tag{3}$$

where M is a collision partner, which is either $S1$ or $S2$ in this case. The source terms for $S1$ and $S2$ can be written using law of mass action

$$w_{S1} = -M_{S1} k_f \frac{\rho_{S1}}{M_{S1}}\left(\frac{\rho_{S1}}{M_{S1}} + \frac{\rho_{S2}}{M_{S2}}\right) + M_{S1} k_b \frac{\rho_{S2}}{M_{S2}}\left(\frac{\rho_{S1}}{M_{S1}} + \frac{\rho_{S2}}{M_{S2}}\right) = w_f + w_b \tag{4}$$

and $w_{S2} = -w_{S1}$; k_f and k_b are forward and backward reaction rates respectively. These are written as

$$k_f = C_f T^\eta e^{-\theta/T}, \qquad k_b = \frac{k_f}{K_{eq}}, \tag{5}$$

where K_{eq} is the temperature-dependent equilibrium constant. For a two species mixture, the diffusion velocity can be accurately represented using Fick's law

$$\rho_s v_{sj} = -\rho D \frac{\partial c_s}{\partial x_j}, \tag{6}$$

where $c_s = \rho_s/\rho$ is the mass fraction, and D is the diffusion coefficient given in terms of the Lewis number

$$Le = \frac{\rho D Pr}{\mu}, \tag{7}$$

where Pr is the Prandtl number, μ is the viscosity which is calculated by Gupta[20]-Yos[21] mixing rule, and Le is taken to be unity, so that the energy transport due to mass diffusion is equal to the energy transport due to thermal conduction.

sectionGoverning Parameters The non-dimensional parameters governing the turbulence chemistry interaction are[14] the turbulent Mach number, the Reynolds number, the Damköhler number, and the relative heat release, namely

$$\begin{aligned} M_t &= \tfrac{q}{a}, & Da &= \frac{\tau_t}{\tau_c} \\ Re_\lambda &= \tfrac{\rho u' \lambda}{\mu}, & \overline{\Delta h^\circ} &= -\frac{\Delta h^\circ}{c_v T + \frac{1}{2} q^2} \end{aligned} \tag{8}$$

where $q = \langle u_i' u_i' \rangle^{1/2}$ is the rms magnitude of the fluctuation velocity; a is the speed of sound; u' is the rms turbulent velocity fluctuation in one direction; λ is the Taylor micro-scale; and Δh° is the heat of the reaction.

The Damköhler number is the ratio of the turbulent time scale τ_t, to the chemical time scale, τ_c and represents a non-dimensional reaction rate; Here $\tau_t = k/\epsilon$, where k and ϵ are the turbulent kinetic energy and dissipation, respectively; $\tau_c = \rho / \left(\langle w_{S1}^2 \rangle^{1/2} \mathrm{K}_{eq} \right)$. A large Damköhler number indicates that chemical reactions are fast relative to turbulent evolution, while a small Damköhler number indicates chemical reactions progress slowly compared with turbulence.

III. Numerical Method

The spatial derivatives are computed using a fourth-order accurate, linearly and non-linearly optimized WENO scheme.[22] This WENO scheme prevents oscillations near shock waves without introducing excessive dissipation and offer high bandwidth resolution in smooth regions. Since the Riemann problem resulting from WENO reconstruction is computationally expensive to solve exactly, an approximate Riemann solver is used. One of the most commonly used approximate Riemann solvers is Roe scheme, which was derived by Roe[23] for perfect gas. For chemically reacting flows, the Roe scheme needs to be generalized to include multicomponent and non-equilibrium effects.[24]

To perform the numerical integration, we use a third-order accurate low-storage Runge-Kutta method by Williamson.[25] The viscous terms are computed using a fourth-order accurate central scheme. An extensive description of code validation is given in Duan & Martin.[26]

IV. Turbulence mechanisms

The chemical reactions act as energy sources within the turbulent boundary layer. Thus, we must address the energy exchange between the turbulence and the chemical reactions. There are four energy exchange mechanisms that take place in turbulent boundary layers: transport, production, dissipation and diffusion of turbulence. The budget equation for the turbulent kinetic energy is

$$\frac{\partial}{\partial t} \bar{\rho} \tilde{k} + \tilde{w} \frac{\partial}{\partial z} \bar{\rho} \tilde{k} = P_k + T_k + \Pi_t + \Pi_d + \phi_{dif} + \phi_{dis} \tag{9}$$

where

$$\begin{aligned} P_k &= -\overline{\rho u_i'' w''} \, \tfrac{\partial \tilde{u}_i}{\partial z} , \\ T_k &= -\tfrac{1}{2} \, \tfrac{\partial}{\partial z} \overline{\rho u_i'' u_i'' w''} , \\ \Pi_t &= -\tfrac{\partial}{\partial z} \overline{w'' p'} , & \Pi_d &= \overline{p' \tfrac{\partial u_i''}{\partial x_i}} , \\ \phi_{dif} &= \tfrac{\partial}{\partial z} \overline{u_i'' \sigma_{iz}'} , & \phi_{dis} &= \overline{\sigma_{ij}' \tfrac{\partial u_i''}{\partial x_j}} , \end{aligned} \tag{10}$$

and P_k is the production due to the mean gradients, T_k is the redistribution of turbulent kinetic energy, Π_t is the pressure diffusion, and Π_d is the pressure dilation, ϕ_{dif} is the viscous diffusion, ϕ_{dis} is the viscous dissipation. There are other terms that appear in the equation due to the Favre averaging, however these terms are negligible. Note that u' and u'' represent fluctuations with respect to the Reynolds and Favre averages of u, respectively.

To study the turbulent internal energy we use the evolution equation for the temperature variance, which is given by

$$\frac{D\overline{T'^2}}{Dt} = P_{ws} + P_{gradT} + \varphi_{tdil} + \varphi_{vdis} + \varphi_{tdif} + \varphi_{tp} + \varphi_{sdif} \tag{11}$$

where

$$\begin{aligned}
P_{ws} &= -\overline{\frac{2}{c_v\rho}T'(\sum_s w_s h_s^\circ)} \\
P_{gradT} &= -2\overline{T'u_j'}\frac{\partial\overline{T}}{\partial x_j} \\
\varphi_{tdil} &= -\overline{2\gamma TT'\frac{\partial u_j}{\partial x_j}} \\
\varphi_{vdis} &= \overline{2\frac{\tau_{ij}}{\rho c_v}\frac{\partial u_i}{\partial x_j}T'} \\
\varphi_{tdif} &= -\overline{2\frac{T'}{\rho c_v}\frac{\partial q_j}{\partial x_j}} \\
\varphi_{tp} &= -\overline{u_j'\frac{\partial T'^2}{\partial x_j}} \\
\varphi_{sdif} &= \overline{2\frac{\gamma}{\rho}\frac{\partial}{\partial x_j}\sum_s(\rho D\frac{\partial c_s}{\partial x_j})TT'}
\end{aligned}$$

and P_{ws} is the production of temperature fluctuations due to the chemical reactions and h° is the heat of formation of species s; P_{gradT} is the production of temperature fluctuations due to mean temperature gradient; φ_{tdil} is the transport of temperature fluctuations due to the temperature-dilatation correlation; φ_{vdis} represents the viscous dissipation of kinetic energy into internal energy; φ_{tdif} is the diffusion of temperature fluctuations due to heat conduction $q_j = -\kappa\partial T/\partial x_j$; and φ_{sdif} is the redistribution of temperature fluctuations due to the diffusion of species, where D is the species diffusivity and c_s is the mass fraction of species s. φ_{tp} is the convection of temperature fluctuation variance due to turbulence fluctuation; The last term, φ_{sdif} is negligible since for our model reaction the gradients of species S1 and S2 are equal in magnitude and opposite in sign.

V. Flow conditions

The boundary layer edge conditions chosen are $Re_\theta = 3023$, $M_e = 4.0$, $T_e = 4210$K, and $\rho_e = 0.49$kg/m3, giving $\delta^+ = 1062$. The wall temperature is chosen to be 4000K. These conditions are characteristic of post-shock conditions of air-breathing vehicles and is high enough to induce chemical reactions in the boundary layer. For this particular condition, the dominant reactions in the air are the dissociation-recombination of oxygen. To simplify the analysis, we use the dissociation-recombination of oxygen, $O_2 + M \rightleftharpoons 2O + M$ to represent the reactions in the air.

The flow field is initialized following the procedure given by Martin.[27] The domain size is $7.1\delta\times2.0\delta\times31.6\delta$ in stream-wise, span-wise, and wall normal directions to enclose a good statistical sample of the larges structures. Here δ is the boundary layer thickness. The grid resolution is $448 \times 304 \times 144$ to resolve all the turbulent scales from large energy containing eddies down to dissipative eddies. Periodic boundary conditions are used in stream-wise and span-wise directions. The species mass fractions are initialized to the their equilibrium values at the averaged temperature in order to isolate the effect of turbulent fluctuations.

Since this initial state is not physical, there will be an initial transient of flow field to physical state. Figure 1 shows the temporal evolution of the friction velocity u_τ. Around $\tau_t = 5$, where τ_t is non-dimensional time unit defined as $\tau_t = tu_\tau/\delta$, u_τ levels off, indicating the onset of equilibrium turbulence in the near-wall region. Figure 2 plots the correlation between velocity fluctuation in stream-wise direction and temperature fluctuation at $\tau_t = 6, 7, 8$, indicating equilibrium of turbulence across the boundary layer. We gather statistics from $\tau_t = 8$ to $\tau_t = 12$. During this period, the displacement thickness δ^* grows less than 5%, indicating the time sampling is much shorter than the time scale for boundary layer growth and the time-developping boundary layer can be viewed as a good approximation of a static boundary layer.

VI. Results and Discussion

A direct numerical simulation of a chemically reacting turbulent boundary layer is performed. For comparison purposes, we also run a simulation beginning from the same initial field but without chemical reactions, as a reference state to show the effect of chemical reactions in the turbulence field.

VI.A. Effect of turbulence on reaction rate

Figure 3 shows the average production rate of oxygen molecule, w_{O_2}. Across the boundary layer, w_{O_2} is negative, indicating the destruction of O_2 or that the dissociation reaction is dominant over the recombination reaction. Figure 4 shows the effects of turbulence fluctuations on reaction rate, where the amplification factor, $\frac{\overline{k(T)}}{k(\overline{T})}$,[28] for reaction rates is introduced. The dissociation reaction rate is amplified by more than 15% due to turbulent fluctuations while the recombination reaction rate hardly changes, indicating different sensitivities of reaction rate to turbulence. This can be explained as follows. The dissociation reaction needs large activation energy to break the chemical bond of oxygen molecules and its reaction rate depends exponentially on temperature, and temperature fluctuations significantly change reaction rate. In contrast, the recombination reaction needs the third body to take away the extra energy and is not temperature limited, so turbulent temperature fluctuations have very subtle influence on its reaction rate.

VI.B. Temperature fluctuation variance $< T'T' >$

Figure 5 plots the normalized temperature fluctuation variance across the boundary layer. Both the the magnitude of mean temperature and temperature fluctuations in the reacting boundary layer is significantly smaller than that for the non-reacting case in most part of boundary layer, indicating that the turbulence has been damped by the chemical reactions. This may be explained by the fact that the overall effects of chemical reactions are endothermic and they act as energy sinks within the turbulent boundary layer. The reduction in the temperature fluctuations is consistent with the findings of Martin and Candler[14] concerning the decay of isotropic turbulence. The contribution of chemical reaction to temperature fluctuation could be further illustrated by using the evolution equation for the temperature variance. Figure 6 plots the budget of the terms in the evolution equation for $< T'T' >_t$, both near the wall and across the boundary layer. Chemical production term P_{ws} has a negative peak at around $z^+ = 5$ and goes gradually to zero when it gets away from the wall.

The contribution of chemical reaction to temperature fluctuation could be further illustrated by using the evolution equation for the temperature variance. Figure 6 plots the budget of the terms in the evolution equation for $< T'T' >_t$, both near the wall and across the boundary layer. Chemical production term P_{ws} has a negative peak at around $z^+ = 5$ and goes gradually to zero when it gets away from the wall. P_{ws} could be split into P_{wf} and P_{wb} to demonstrate the contributions due to dissociation reaction w_f and recombination reaction w_b respectively, which are shown in Figure 7. P_{wf} is negative and P_{wb} is positive, indicating the dissociation reaction damps turbulence while the recombination reaction enhances turbulence. Also, the absolute value of P_{wf} is significantly larger than P_{wb} near the wall, indicating that the effect of the dissociation reaction is dominant near the wall. Figure 6 also shows that the temperature dilation term φ_{tdil} in Eq. 11 is dominant across the boundary layer except very near the wall, where viscous dissipation φ_{vdis} and thermal diffusion due to heat conduction φ_{tdif} are dominant. This indicates that chemical reactions influence turbulence fluctuations by the heat of reaction which causes volumetric flow expansion/contraction, which is consistent with the previous findings.[14,16]

VI.C. Reynolds stresses and TKE budget

Figure 8 plots the non-dimensional stream-wise, span-wise, wall-normal and shear Reynolds stresses across the boundary layer. Figure 9 plots the non-dimensional turbulent kinetic energy across the boundary layer. With chemical reactions, both Reynolds stresses and turbulent kinetic energy increases. Figure 10 plots the non-dimensional turbulent kinetic energy (TKE) budget both near the wall and across the boundary layer. With chemical reactions, every term in the evolution equation of TKE budget has an increase in the peak value, and the location of the peak shifts toward the wall relative to the non-reacting case. As endothermic reactions are dominant, the average temperature decreases significantly across the boundary layer 5b relative to the non-reacting case. Since the wall temperature remains unchanged, the temperature

gradient decreases near the wall and the turbulence mixing will be enhanced by the steeper turbulence structures, as it is observed in turbulent boundary layer heat-transfer studies.[29] Figure 11 shows a better collapse of data when using a coordinate transformation that takes into account the variation in density and temperature across the boundary layer. This transformation is given by $\zeta^+ = \int_0^z \frac{<\rho> u_\tau}{<\mu>} dz$. The location of maximum and minimum values of the budget terms is nearly the same for reacting and non-reacting cases. It is shown that the production term is larger for the reacting case across the layer. This is further evidence of the increased turbulence mixing due to the change in the temperature profile. Additional turbulence structure analysis are desirable. The pressure-dilation remains relatively unchanged.

VI.D. Turbulence-chemistry interaction

Figure 12 shows the normalized magnitude of the fluctuations in temperature and mass fraction of O_2 across the reacting boundary layer. Both the temperature fluctuation and species concentration fluctuation profiles have two peaks, and the peak locations for the two profiles are nearly the same, with one near the wall and the other near $z/\delta = 0.9$. The similarity in the two profiles indicates a strong turbulence-chemistry interaction. In addition, it can be seen that the maximum temperature fluctuation is a bit less than 5% of the average, while the maximum species concentration fluctuation is more than 30% of the average, indicating that a relative small temperature fluctuation would cause a large fluctuation in chemical composition.

To further illustrate turbulence-chemistry interaction effects, Figure 13 plots the correlation between temperature fluctuation and mass fraction fluctuation of O_2. When chemical reactions are introduced, the correlation increases significantly, especially near the wall around the peaks of $< T'T' > / < T >$ and $< c'c' > / < c >_{O_2}$, indicating the strongest interaction happens near the wall, in the buffer layer of the boundary layer for this particular condition.

VII. Conclusion

In the hypersonic boundary layer, turbulent fluctuations have different influence on recombination and dissociation reactions. For the conditions chosen, temperature fluctuations significantly amplify the rate of dissociation. In contrast, the rate of recombination reaction is nearly unchanged due to temperature fluctuation. Recombination reaction enhances the magnitude of temperature fluctuations, while dissociation reaction has the opposite effect. For this particular condition, the net effect of forward and backward reactions is to damp the magnitude of temperature fluctuations. Temperature fluctuations cause large fluctuations in species composition. Chemical reactions have a subtle influence of the TKE. The dominant forward (endothermic) reaction changes the temperature profile, which influences the turbulence mixing while enhancing turbulence production.

VIII. Acknowledgment

This work is sponsored by the Air Force Office of Scientific Research under Grant FA9550-05-1-0490 and NASA under Grant NNX08AD04A.

References

[1]Pope, S., "Computations of turbulent combustion: Progress and challenges," *Proceedings of 23rd Symposium (Int.) on combustion (The Combustion Institute, Pittsburgh, PA)*, 1990, pp. 591–612.

[2]Libby, P. and Williams, F., "Turbulent reacting flows," *Academic, London*, 1994.

[3]Vervisch, L. and Poinsot, T., "Direct numerical simulation of non-premixed turbulent flames," *Annu. Rev. Fluid Mech.*, Vol. 330, 1998, pp. 655.

[4]Baurle, R. and Girimaji, S., "Assumed PDF turbulence-chemistry closure with temperature-composition correlations," *Combustion and Flames*, Vol. 134, 2003, pp. 131–148.

[5]McMurtry, P., Jou, W., Riley, J., and Metcalfe, R., "Direct numerical simulations of a reacting mixing layer with chemical heat release," *AIAA J.*, Vol. 24, 1986, pp. 962.

[6]McMurtry, P., Riley, J., and Metcalfe, R., "Effects of heat rlease on the large scale structures in a turbulent reacting mixing layer," *Journal of fluid mechanics*, Vol. 199, 1989, pp. 33.

[7]Givi, P., "Model free simulations of turbulent reactive flows," *Prog. Energy Combust. Sci.*, Vol. 15, No. 1, 1989.

[8]Hermanson, J. and Dimotakis, P., "Effects of heat release in a turbulent, reacting shear layer," *Journal of fluid mechanics*, Vol. 199, 1989, pp. 333–375.

[9]Dimotakis, P., "Turbulent free shear layer mixing and combustion," *High speed flight propulsion systems, Progress in astronautics and aeronautics, AIAA, Washington D.C.*, Vol. 137, 1991, pp. 265–340.

[10]Coats, C., "Coherent structures in combustion," *Prog. Energy Combust. Sci.*, Vol. 22, 1996, pp. 427.

[11]Eschenroeder, A., "Intensification of turbulence by chemical heat release," *Physics. fluids*, Vol. 7, 1964, pp. 1735.

[12]Hill, J., "Homogeneous turbulent mixing with chemical reaction," *Annu. Rev. Fluid Mech.*, Vol. 8, 1976, pp. 135.

[13]Jaberi, F. and Madnia, C., "Effects of heat of reaction on homogeneous compressible turbulence," *J. Sci. Comput.*, Vol. 13, 1998, pp. 201.

[14]Martin, M. and Candler, G., "Effect of Chemical Reactions on Decaying Isotropic Turbulence," *Physics of Fluids*, Vol. 10, No. 7, 1998, pp. 1715–1724.

[15]Bakakrishnan, G., Sarkar, S., and Williams, F., "Direct numerical simulation of diffusion flames with large heat release in compressible homogeneous turbulence," *AIAA Paper, 95-2375*, 1995.

[16]Jaberi, F., Livescu, D., and Madnia, C., "Charateristics of chemically reacting compressible homogeneous turbulence," *Physics of Fluids*, Vol. 12, No. 5, May 2000, pp. 1189–1209.

[17]Martin, M. and Candler, G., "DNS of Mach 4 boundary layer with chemical reactions," *AIAA Paper No.2000-0399*, 2000.

[18]M.P.Martin and Candler, G., "Temperature Fluctuation Scaling in Reacting Turbulent Boundary Layers," *AIAA Paper No.01-2717*, 2001.

[19]Martin, M., "Exploratory Studies of Turbulence/Chemistry Interation in Hypersonic Flows," *AIAA Paper No. 03-4055*, 2003.

[20]Gupta, R., Yos, J., Thompson, R., and Lee, K., "A Review of Reaction Rates and Thermodynamic and Transport Properties for 11-Species Air Model for Chemical and Thermal Nonequilibrium Calculations to 30000K," *NASA RP-1232*, 1990.

[21]Yos, J., "Transport properties of nitrogen, hydrogen, oxygen, and air to 30,000 K," *Avco. Corp. TR AD-TM-63-7*, 1963.

[22]Taylor, E., Wu, M., and Martin, M., "Optimization of Nonlinear Error Sources for Weighted Non-Oscillatory Methods in Direct Numerical Simulations of Compressible Turbulence," *Journal of Computational Physics*, Vol. 223, 2006, pp. 384–397.

[23]P.L.Roe, "Approximate Riemann solvers, parameter vectors, and difference schemes," *Journal of Computational Physics*, Vol. 43, 1981, pp. 357–372.

[24]an M. Vinokur, Y. L., "Upwind algorithms for general thermo-chemical nonequilibrium flows," *AIAA paper No. 1989-0201*, 1989.

[25]Williamson, J., "Low-storage Runge-Kutta Schemes," *Journal of Computational Physics*, Vol. 35(1), 1980, pp. 48–56.

[26]Duan, L. and Martin, M., "Procedure to Validate Direct Numerical Simulations of Wall-Bounded Turbulence Including Finite-Rate Reactions," *AIAAJ*, Vol. 47, No. 1, 2009.

[27]Martin, M., "DNS of Hypersonic Turbulent Boundary Layers. Part I: Initialization and Comparison with Experiments," *Journal of Fluid Mechanics*, Vol. 570, 2007, pp. 347–364.

[28]Gaffney, R., White, J., Girimaji, S., and Drummond, J., "Modeling turbulent/chemistry interactions using assumed PDF Methods," *AIAA Paper No. 1992-3638*, 1992.

[29]Beekman, I., Priebe, S., Ringuette, M., and Martin, M., "Effect of wall temperature and Mach number on the turbulence structure of hypersonic boundary layer," *AIAA Paper, 2009-1328*, 2009.

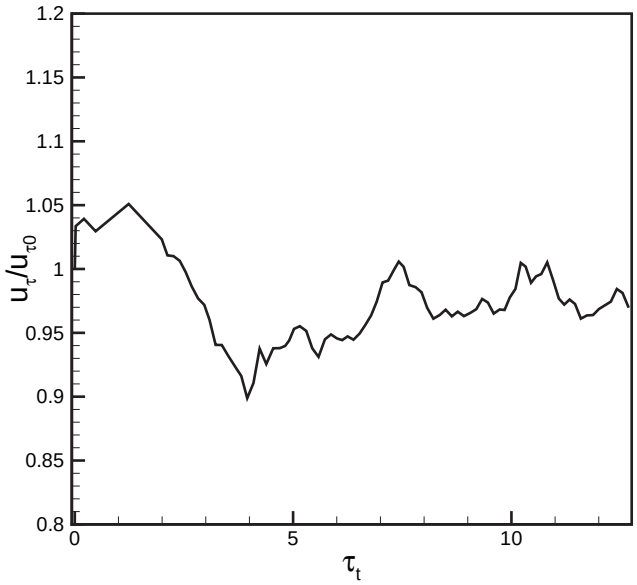

Figure 1. Temporal evolution of the normalized friction velocity

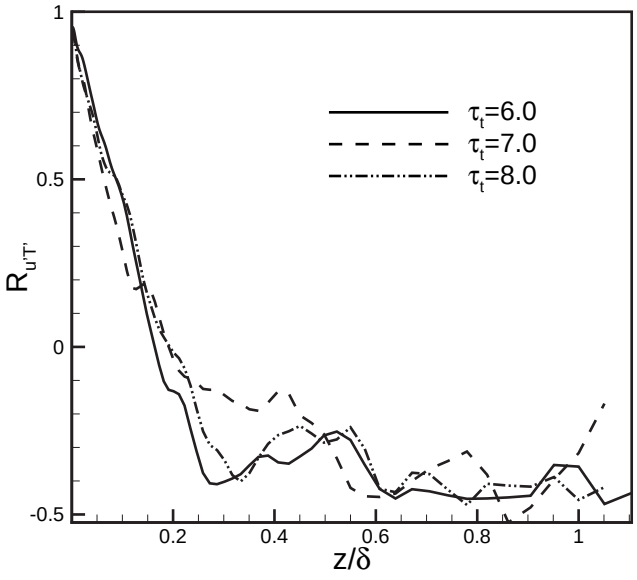

Figure 2. Correlation of stream-wise velocity fluctuation and temperature fluctuation across the boundary layer at different time instances

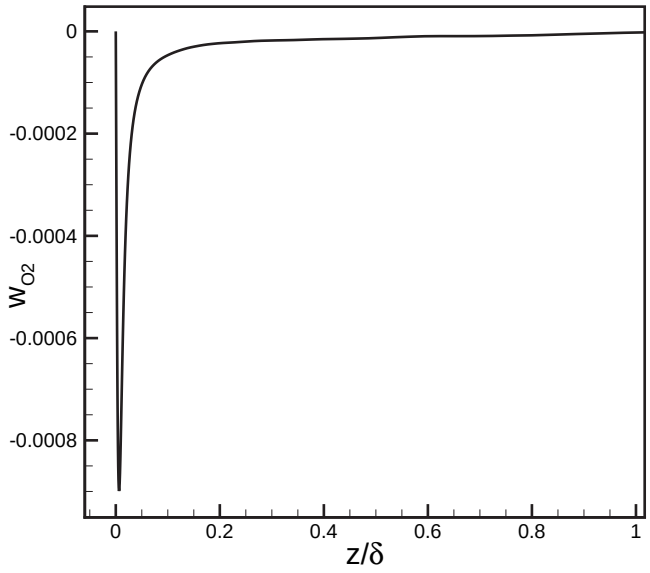

Figure 3. The production rate of oxygen molecules across the boundary layer

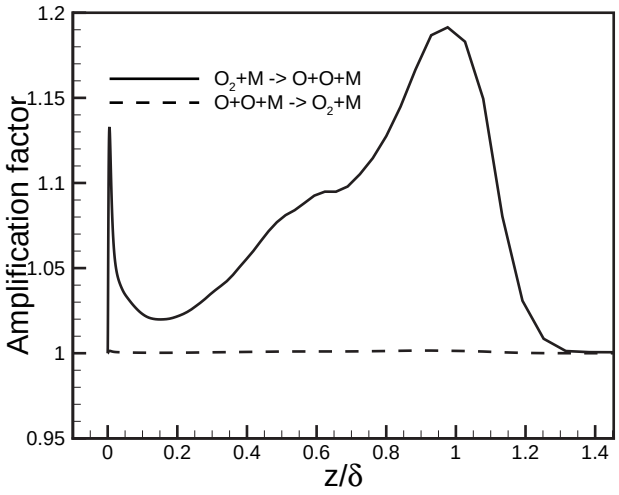

Figure 4. The amplification factor, $\frac{\overline{k(T)}}{k(\overline{T})}$,[28] across the boundary layer

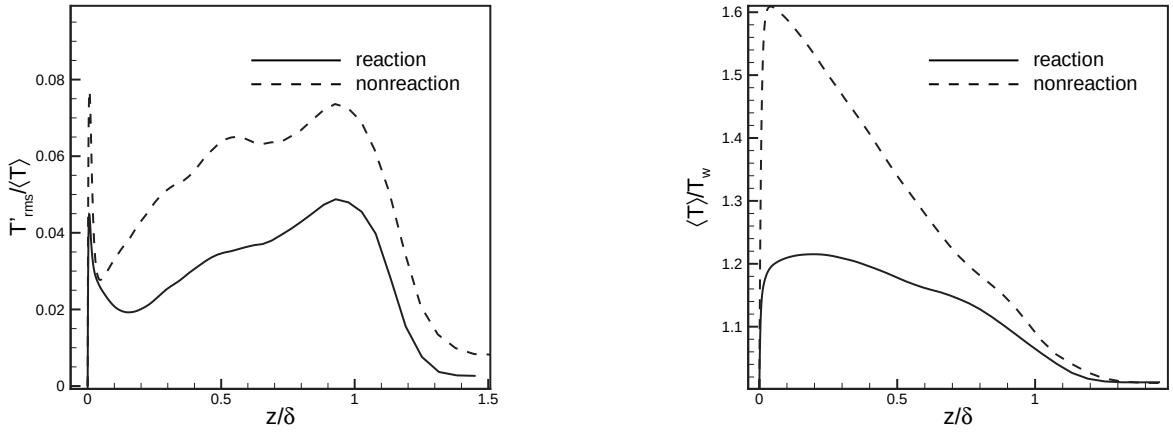

(a) (b)

Figure 5. (a) **Normalized magnitude of temperature fluctuation variance** $< T'T' > / < T >$ **and** (b) **mean temperature** $< T > / < T_w >$ **across the boundary layer.**

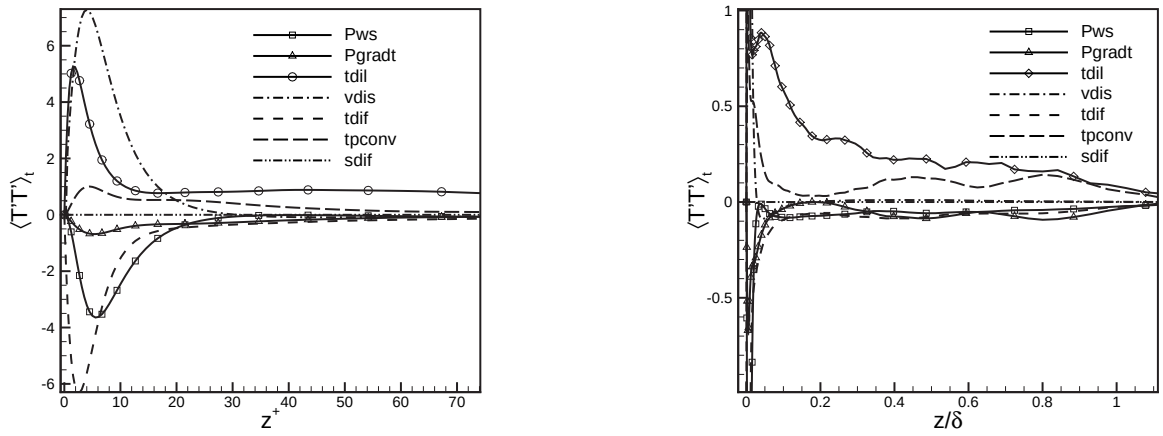

(a) (b)

Figure 6. Budget of the terms in the evolution equation for $< T'T' >_t$ (a) **near the wall and** (b) **across the boundary layer. The terms are normalized using** $u_\tau^5/C_v^2 z_\tau$**.**

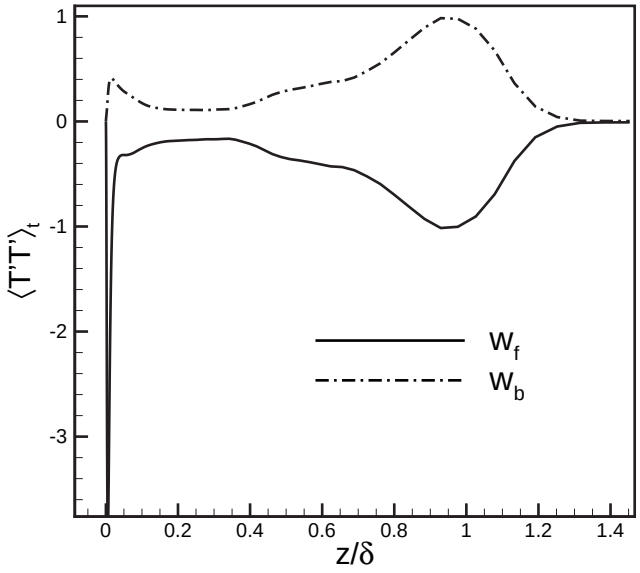

Figure 7. Contribution of chemical production to $< T'T' >_t$. The terms are normalized using $u_\tau^5/C_v^2 z_\tau$.

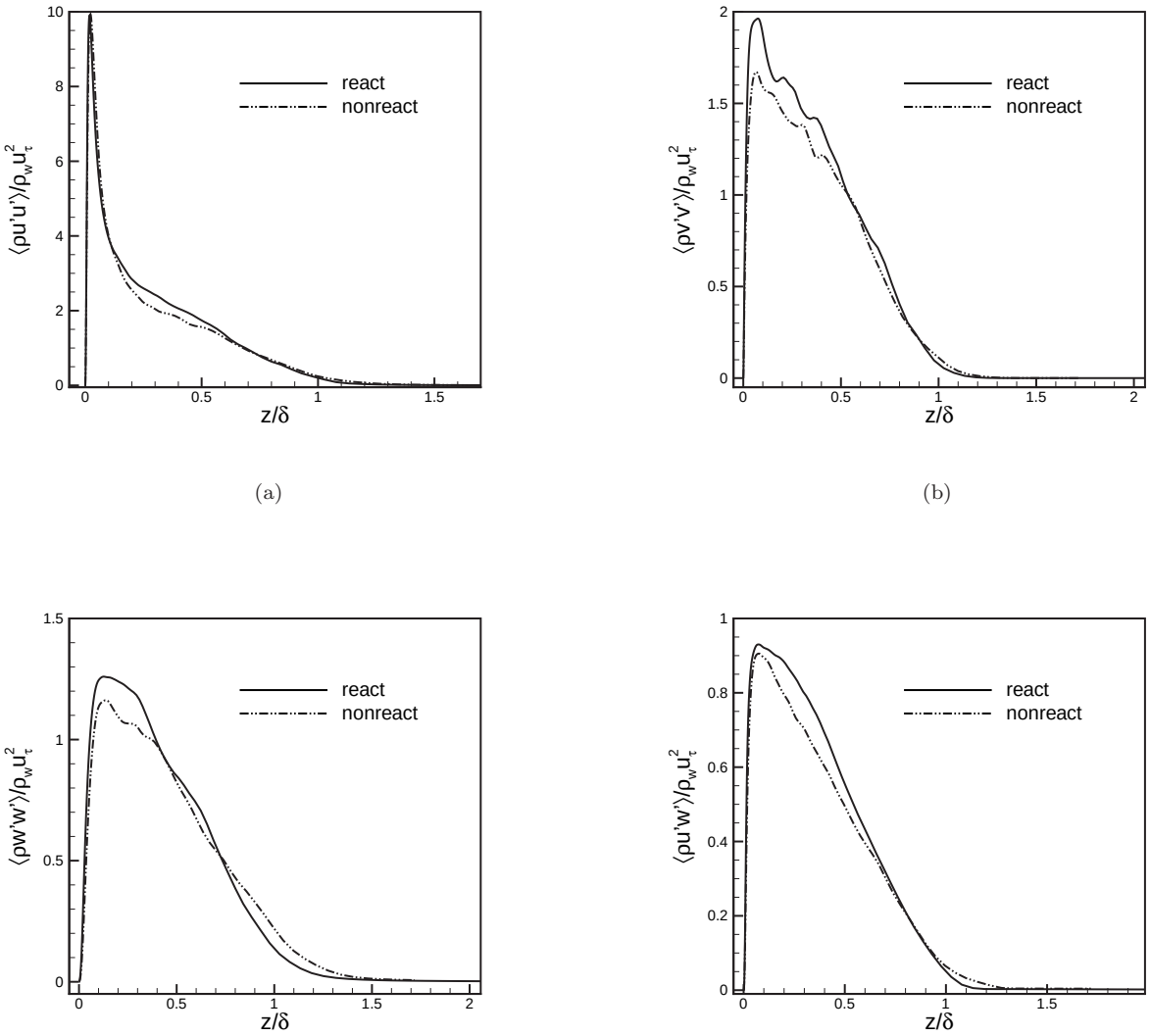

Figure 8. Non-dimensional (a) stream-wise, (b) span-wise, (c) wall-normal, and (d) shear Reynolds stresses across the boundary layer.

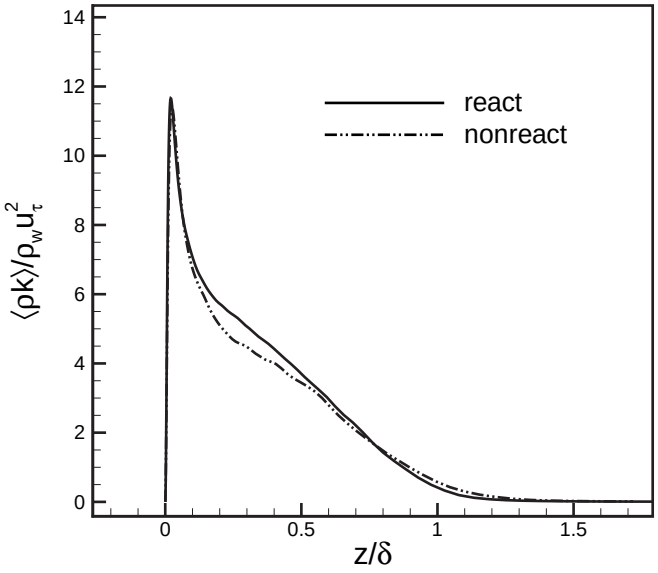

Figure 9. Non-dimensional turbulent kinetic energy across the boundary layer

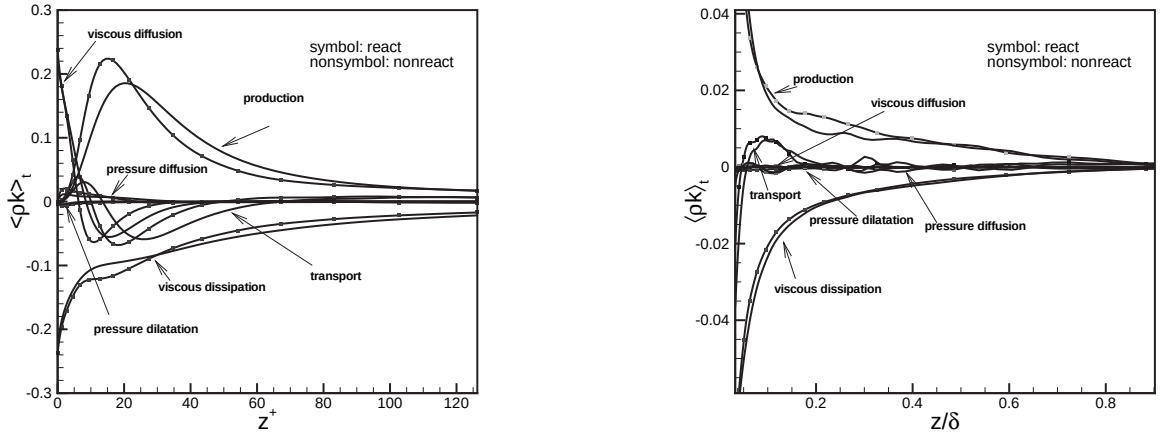

(a) (b)

Figure 10. Budget of the terms in the evolution equation for $< \rho k >_t$ (a) near the wall and (b) across the boundary layer. The terms are normalized using $\rho_w u_\tau^3 / z_\tau$.

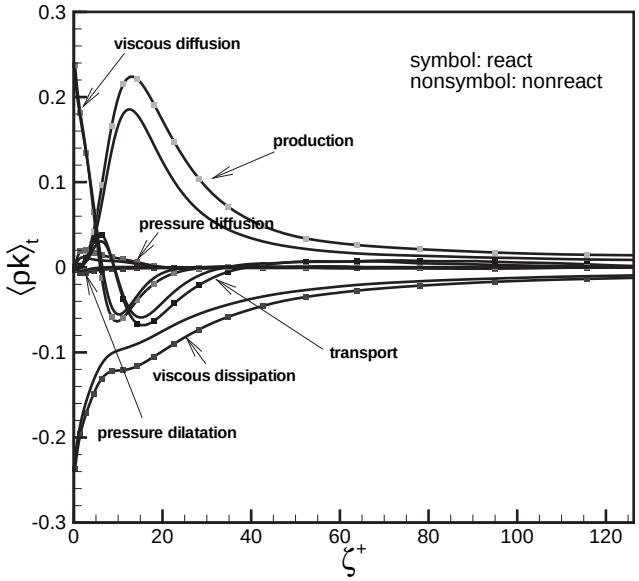

Figure 11. Budget of the terms in the evolution equation for $< \rho k >_t$ versus ζ^+. The terms are normalized using $u_\tau^5/C_v^2 z_\tau$.

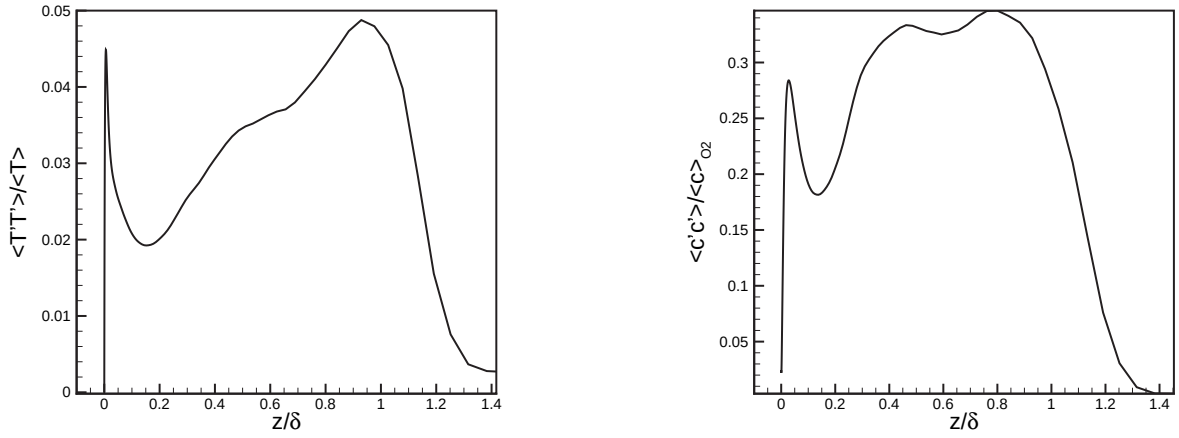

(a) (b)

Figure 12. Normalized magnitude of the fluctuations in (a) temperature and (b) mass fraction of O_2

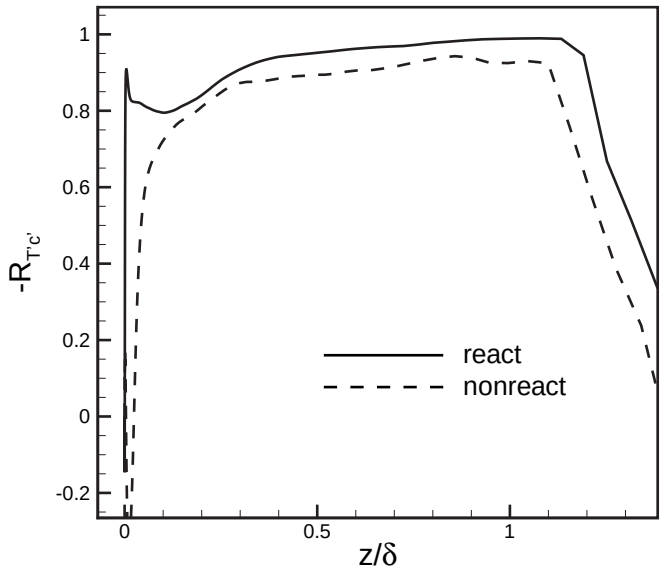

Figure 13. Correlation of the temperature fluctuation and O_2 mass fraction fluctuation across the boundary layer for both reaction and non-reaction cases